International Journal of Engineering Research & Technology (IJERT)
ISSN: 2278-0181
Vol. 15 Issue 08 , August - 2026

Dual-Function Rectangular Microstrip Patch Antenna for Non-Invasive Kidney Stone Sensing and 2.4 GHz WLAN Integration

Sk. Shakeer[1], K. Manasa[1], J. Lokesh[1], B. Suraj[1], K. Arshiya[1], K. Srinivasa Rao[2]
[1]UG Scholar, Department of Electronics and Communication Engineering, JNTUA College of Engineering, Anantapur, Andhra Pradesh, India
[2]Assistant Professor (Adhoc), Department of Electronics and Communication Engineering, JNTUA College of Engineering, Anantapur, Andhra Pradesh, India

Abstract - Kidney stones remain a widespread urological condition, and their timely, reliable detection is important for preventing complications; however, conventional imaging modalities carry known limitations, from noise-prone ultrasound scans to the radiation exposure associated with CT imaging. This work presents a compact rectangular microstrip patch antenna designed to resonate at 2.4 GHz for two purposes at once: non-invasive kidney stone sensing through microwave reflection, and standard WLAN connectivity. The antenna, etched on an FR-4 substrate with an inset feed for 50 Ω impedance matching, was modelled and analysed in CST Studio Suite and evaluated against a seven-layer anatomical kidney phantom that replicates human skin, fat, muscle, renal capsule and kidney tissue. In free space the antenna delivered a gain of 6.019 dBi, a bandwidth of 47.6 MHz and a radiation efficiency of 93.9%. When stones of increasing size were embedded in the phantom, the return loss (S11) deepened progressively, from −36.95 dB in the stone-free case to −38.76 dB for the largest modelled stone, giving a measurable 1.81 dB diagnostic shift. The design also satisfied WLAN impedance requirements and remained within safe exposure limits, recording a Specific Absorption Rate of 1.95 W/kg. The results indicate that a single antenna structure can support biomedical sensing and wireless communication without compromising either function.

Key Words: Microstrip Patch Antenna, Kidney Stone Detection, Microwave Imaging, WLAN, S-Parameter, Specific Absorption Rate.

1. INTRODUCTION

Kidney stone disease is one of the more common disorders encountered in urology, and its clinical management depends heavily on how early and how accurately the stones can be located. Ultrasound remains the most widely used first-line tool because it avoids ionising radiation, but its images are prone to speckle noise and operator-dependent variability, which can obscure small or early-stage stones. Computed tomography offers sharper resolution but exposes the patient to radiation, making it unsuitable for repeated monitoring. These trade-offs have motivated interest in microwave-based sensing as a complementary or alternative diagnostic route, since it is non-ionising, potentially low-cost, and can be implemented with compact, planar hardware [3].

A microwave sensing approach depends on the fact that biological tissues and kidney stones have markedly different dielectric properties at a given frequency, so a signal reflected from a stone-bearing region carries a detectable signature. Realising this in practice, however, requires an antenna that behaves predictably both in open air and when placed against, or close to, lossy human tissue — two very different electromagnetic environments. Antenna design for this dual context must therefore account not only for radiation performance but also for detuning caused by tissue loading and for compliance with human exposure safety limits [3, 6].

International Journal of Engineering Research & Technology (IJERT)
ISSN: 2278-0181
Vol. 15 Issue 08 , August - 2026

A further practical consideration is that most reported biomedical sensing antennas are built for a single task. Devices proposed for kidney cancer or kidney stone sensing are rarely evaluated for anything beyond diagnostic use, while antennas built for the 2.4 GHz WLAN band are optimised purely for communication metrics such as gain and bandwidth [5]. A closely related study by Sadat and Hossan reported a rectangular microstrip patch antenna for combined kidney stone detection and WLAN operation at 2.4 GHz [2]. The present work builds on that general direction but differs in scope: it develops a seven-layer anatomically detailed kidney phantom rather than a simplified tissue model, characterises the antenna response across multiple stone sizes rather than a single stone condition, and benchmarks the resulting gain, efficiency and SAR figures against several previously reported kidney-sensing antennas rather than reporting performance in isolation.

The specific objectives of this study are to: (i) design a compact rectangular microstrip patch antenna resonant at 2.4 GHz on a low-cost FR-4 substrate; (ii) construct a multi-layer kidney phantom that reproduces the dielectric behaviour of skin, fat, muscle and renal tissue; (iii) quantify how the presence and size of a kidney stone shifts the antenna's return loss, VSWR and efficiency; and (iv) confirm that the design meets WLAN impedance requirements and IEEE SAR safety limits so that it can plausibly serve both functions without redesign.

2. LITERATURE REVIEW

Early work on antenna-based renal sensing focused mainly on cancer rather than stone detection. Elshafiey et al. proposed a compact implantable monopole antenna operating in the Medical Implant Communication Service (MICS) band for early-stage kidney cancer detection, demonstrating that implantable or near-body antennas could pick up tissue-level anomalies through S-parameter monitoring, though at a frequency far removed from the ISM band [7]. Islam et al. extended this idea using a circularly polarised patch array operating at 2.4 GHz to differentiate between stages of kidney cancer, showing that the ISM band itself is viable for renal sensing while achieving a reported gain of 6.6 dBi, albeit with a considerably larger footprint than a conventional single-patch design [8].

For stone detection specifically, Al-Gburi et al. introduced a raspberry-shaped ultra-wideband monopole antenna intended for microwave-imaging-based kidney stone screening, operating across 3–11 GHz with a moderate gain of about 5 dBi [4]. Mahbub and Islam instead used a cylindrical dielectric resonator antenna (CDRA) operating near 3.77 GHz, reporting a gain of 5.95 dBi and 89% efficiency for early-stage stone detection based on performance-parameter analysis rather than direct S11 shift monitoring [1]. Across this body of work, a recurring theme is that stone-sensing antennas tend to operate outside the common WLAN band, which limits their reuse for communication purposes.

On the communication side, conventional 2.4 GHz microstrip patch antennas designed purely for WLAN, such as the design reported by Karthick, typically report modest gain and efficiency figures (around 4.7 dBi and 74% efficiency) because their geometry is optimised for impedance matching in free space rather than for sensing sensitivity in a lossy medium [5]. Human exposure safety for any antenna operated close to the body is governed by the IEEE C95.1 standard, which caps the Specific Absorption Rate at 2 W/kg for controlled and uncontrolled environments and forms the benchmark against which any near-body biomedical antenna must be validated [6]. Antenna geometry and feed design in this work follow standard microstrip patch design theory as established by Balanis [3].

Taken together, the literature indicates two largely separate design traditions — one for renal/biomedical sensing and one for WLAN communication — with comparatively few designs validated for both roles simultaneously. This gap motivates the dual-purpose antenna developed in the present study, which is evaluated against both sets of criteria within a single, consistent simulation framework.

3. PROPOSED METHODOLOGY

3.1 Simulation Environment

International Journal of Engineering Research & Technology (IJERT)
ISSN: 2278-0181
Vol. 15 Issue 08 , August - 2026

All electromagnetic modelling in this study was carried out in CST Studio Suite, a full-wave 3D electromagnetic solver widely used for antenna and biomedical exposure analysis. The software's Finite Integration Technique (FIT) solver supports accurate discretisation of both simple planar antenna geometries and complex multi-layer tissue volumes within the same simulation domain, which made it well suited to bridging the antenna model and the kidney phantom in a single run. The Time Domain Solver was selected for this work because it computes broadband S-parameter and VSWR behaviour across the full 2–3 GHz sweep in one simulation pass, which is more efficient than a frequency-domain approach when repeated parametric adjustments are required.

Fig. 1: CST Studio Suite project workspace used for the antenna and phantom simulations.
Source: Simulation screenshot generated by the authors in CST Studio Suite (2026).

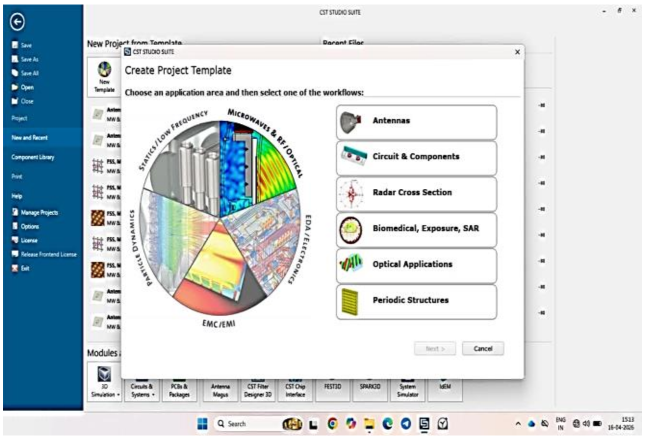

Fig. 2: Project template selection stage in CST Studio Suite, with the Antennas workflow chosen for this design.
Source: Simulation screenshot generated by the authors in CST Studio Suite (2026).

3.2 Antenna Design Procedure

The patch dimensions were obtained from standard microstrip antenna design equations before being fine-tuned through parametric sweeps in CST. FR-4 (lossy) was chosen as the substrate on account of its low cost and adequate dielectric performance at 2.4 GHz, with a relative permittivity of 4.3 and thickness of 1.5 mm; copper was used for the patch, ground plane and feed line at a conductor thickness of 0.035 mm. The design sequence followed the standard transmission-line model [3]:

Free-space wavelength: $\lambda = c / f = (3 \times 10^8) / (2.4 \times 10^9) \approx 125$ mm

Patch width: $W = c / [2f \sqrt{((\varepsilon r + 1)/2)}] \approx 29.25$ mm

Effective dielectric constant: $\varepsilon eff = (\varepsilon r + 1)/2 + (\varepsilon r - 1)/2 \times (1 + 12h/W)^{-1/2} \approx 3.92$

Fringing-field extension: $\Delta L = 0.412h(\varepsilon eff + 0.3)(W/h + 0.264) / [(\varepsilon eff - 0.258)(W/h + 0.8)] \approx 0.71$ mm

Patch length: $L = c / (2f\sqrt{\varepsilon_{eff}}) - 2\Delta L \approx 22.68$ mm, subsequently optimised to 47 mm through iterative impedance-matching sweeps in CST.

An inset feed was used to achieve the target 50 Ω input impedance without requiring an external matching network, and the ground plane was kept continuous beneath the substrate to suppress back radiation. The final optimised patch measured 47 × 29.25 mm on a 1.54 mm-thick substrate.

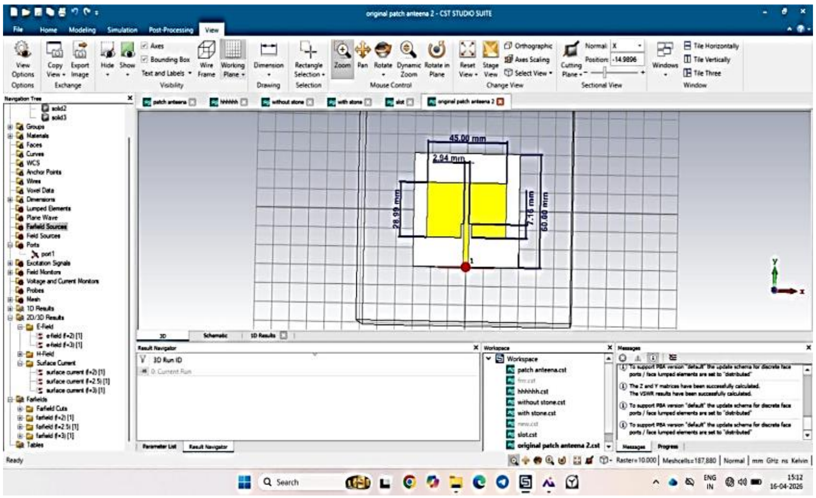

Fig. 3: Layout of the proposed rectangular microstrip patch antenna with inset feed, as modelled in CST Studio Suite.
Source: Simulation screenshot generated by the authors in CST Studio Suite (2026).

3.3 Multi-Layer Kidney Phantom

To evaluate the antenna under realistic loading conditions, a seven-layer anatomical phantom was built to approximate the signal path from the body surface to the kidney: a 2 mm skin layer, a 14 mm muscle layer, 11 mm and 2 mm fat and fascia layers, a 0.3 mm renal capsule, a 21 mm kidney volume of approximately 110 cm^3, and an associated ureter structure. Each layer was assigned frequency-dependent permittivity and conductivity values representative of human tissue at 2.4 GHz; the kidney layer itself was set to a relative permittivity of 52.9, while an embedded stone was modelled with a much lower relative permittivity of 3, creating the dielectric contrast that the sensing mechanism relies on.

The antenna was positioned 71.5 mm from the phantom surface, a separation chosen to keep the antenna within the near-field diagnostic range while maintaining stable coupling to the tissue stack. Detection in this configuration relies on the fact that a kidney stone, having a dielectric constant very different from the surrounding kidney tissue, behaves as a localised reflector: a fraction of the incident 2.4 GHz signal is reflected back toward the antenna, and this fraction changes measurably with stone size, which is captured as a shift in the S11 return-loss trace.

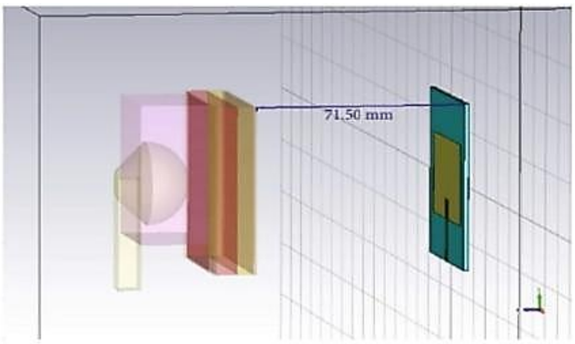

Fig. 4: Antenna-to-phantom separation (71.5 mm) used in the diagnostic simulation scenarios.
Source: Simulation screenshot generated by the authors in CST Studio Suite (2026).

International Journal of Engineering Research & Technology (IJERT)
ISSN: 2278-0181
Vol. 15 Issue 08 , August - 2026

Four simulation scenarios were run under identical solver settings (2–3 GHz sweep, open/add-space boundary conditions, waveguide port excitation at the 50 Ω feed): the antenna alone in free space; the antenna against the stone-free phantom; the phantom with a small embedded stone; and the phantom with a larger embedded stone. Parametric sweeps of patch length, inset feed depth and substrate thickness were used to keep S11 below −27.55 dB at 2.4 GHz across these scenarios.

4. RESULTS AND DISCUSSION

The antenna was evaluated across the four scenarios described in Section 3.3, with VSWR, radiation efficiency and S11 tracked in each case to assess both its WLAN suitability and its sensitivity to the presence of a kidney stone.

4.1 Impedance Matching (VSWR)

VSWR close to unity indicates that almost all incident power is delivered into the antenna rather than reflected back to the source. In free space the antenna recorded a VSWR of approximately 1.09 at 2.4 GHz (Fig. 5), confirming good impedance matching for standard WLAN operation. When the antenna was loaded by the stone-free kidney phantom, dielectric loading from the tissue stack shifted the matching slightly, with VSWR rising to approximately 1.87 while remaining well below the generally accepted threshold of 2 (Fig. 6). With a stone embedded in the phantom, a further, distinguishable shift in the VSWR minimum was observed (Fig. 7), consistent with the additional dielectric discontinuity the stone introduces into the near-field region. The consistent, monotonic pattern across the three cases supports the use of VSWR as a secondary indicator alongside S11 for distinguishing stone-affected from healthy tissue.

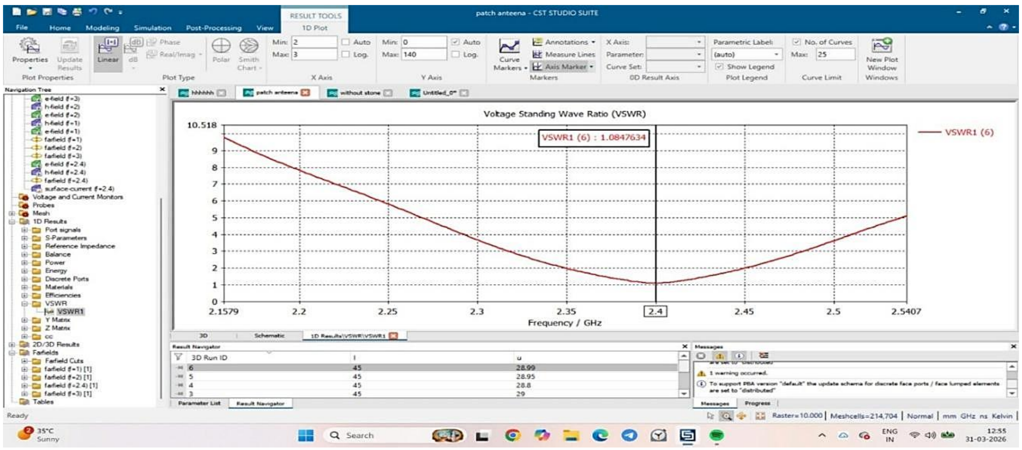

Fig. 5: VSWR of the proposed antenna in free space.

Source: Simulation result generated by the authors in CST Studio Suite (2026).

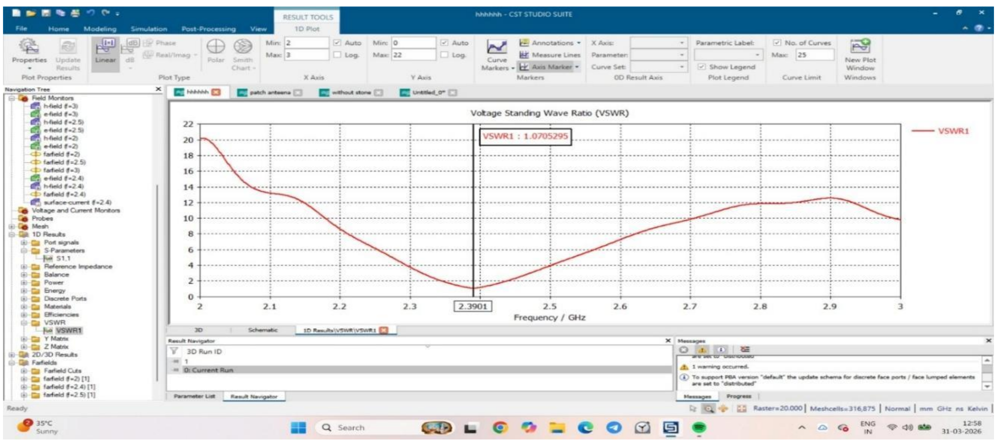

Fig. 6: VSWR with the antenna loaded by the stone-free kidney phantom.

Source: Simulation result generated by the authors in CST Studio Suite (2026).

International Journal of Engineering Research & Technology (IJERT)
ISSN: 2278-0181
Vol. 15 Issue 08 , August - 2026

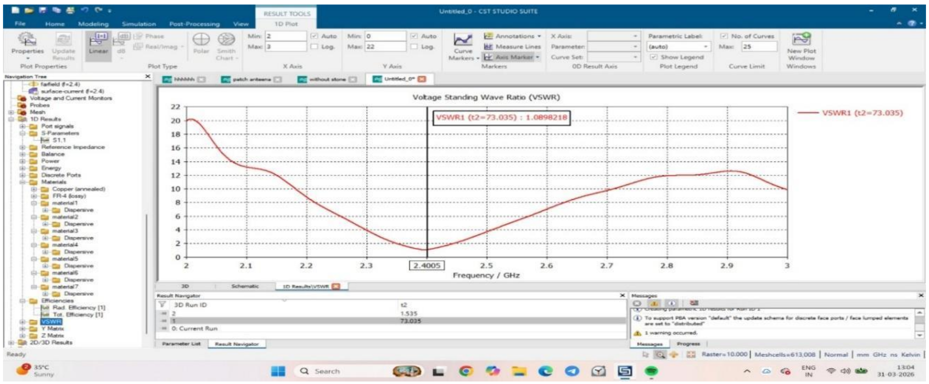

Fig. 7: VSWR with a kidney stone embedded in the phantom.

Source: Simulation result generated by the authors in CST Studio Suite (2026).

4.2 Radiation Efficiency

Radiation efficiency reflects the proportion of input power that is actually radiated rather than dissipated in conductor, dielectric or tissue losses. The antenna reached its highest efficiency, 93.9%, in free space (Fig. 8), where no lossy biological material surrounds the radiating structure. Once the phantom was introduced, efficiency dropped, as expected, because tissue layers absorb part of the radiated energy (Fig. 9); this reduction is an unavoidable consequence of operating close to lossy media rather than a design shortcoming. Comparing the stone-free and stone-affected cases (Figs. 9 and 10) shows a further, measurable change in efficiency attributable to the stone's dielectric discontinuity, reinforcing that efficiency, like S11 and VSWR, carries diagnostic information about the presence of a stone.

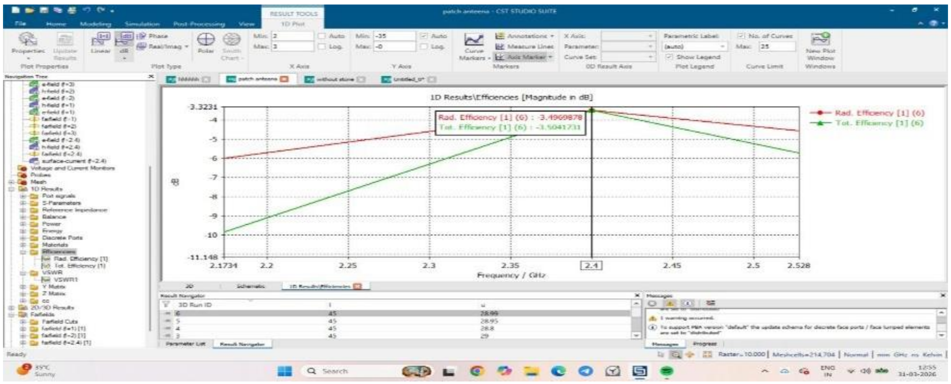

Fig. 8: Radiation and total efficiency of the antenna in free space.

Source: Simulation result generated by the authors in CST Studio Suite (2026).

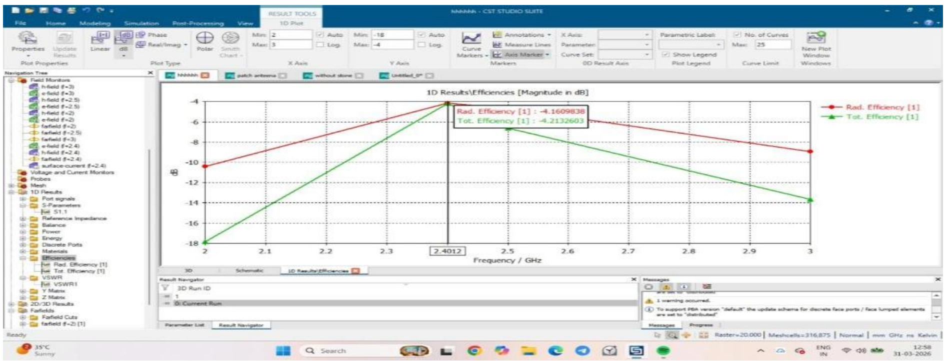

Fig. 9: Radiation and total efficiency with the stone-free kidney phantom.

Source: Simulation result generated by the authors in CST Studio Suite (2026).

International Journal of Engineering Research & Technology (IJERT)
ISSN: 2278-0181
Vol. 15 Issue 08 , August - 2026

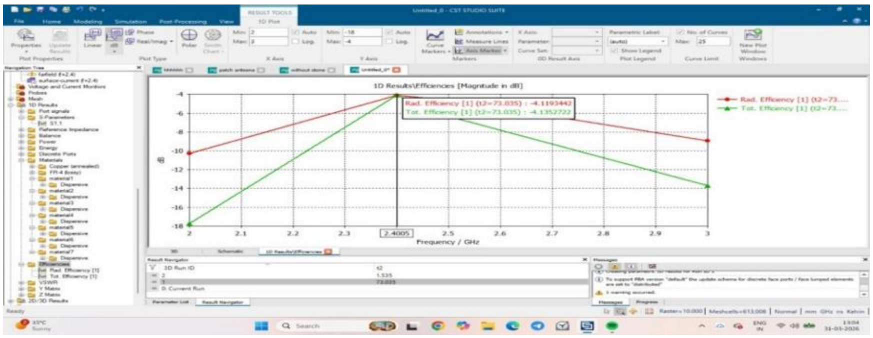

Fig. 10: Radiation and total efficiency with a kidney stone present in the phantom.

Source: Simulation result generated by the authors in CST Studio Suite (2026).

4.3 S-Parameter (S11) Analysis

The S11 return-loss trace is the primary diagnostic signal in this design. In free space the antenna resonated cleanly at 2.4 GHz with S11 = −27.55 dB (Fig. 11), confirming suitability for WLAN-band operation on its own. Against the stone-free phantom, the return loss deepened to −36.95 dB (Fig. 12), a change driven by dielectric loading from the kidney tissue altering the near-field coupling between the antenna and the biological medium. With a small stone embedded in the phantom, S11 deepened further to −38.21 dB, and with a larger stone it reached −38.76 dB (Fig. 13).

This progressive deepening of S11 with increasing stone size — a maximum shift of 1.81 dB between the stone-free and largest-stone conditions — is the diagnostic signature the design relies on. Because the trend is monotonic with stone size rather than merely present-or-absent, the same measurement in principle offers a rough indication of relative stone size, not just stone presence, which is a useful property for a screening-oriented sensor even though it would need experimental confirmation on physical phantoms before any clinical interpretation.

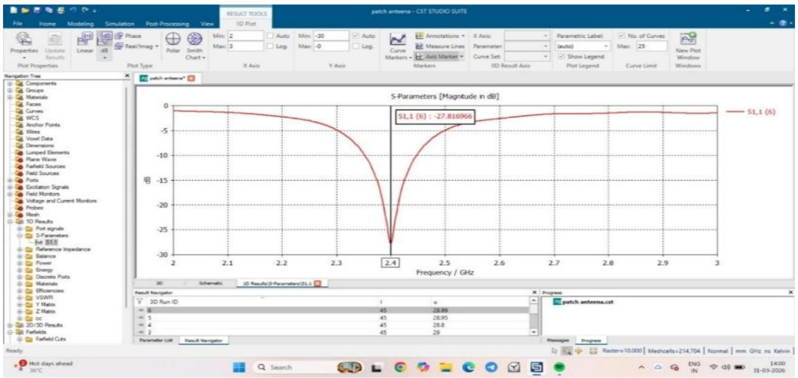

Fig. 11: S-parameter (S11) response of the antenna in free space.

Source: Simulation result generated by the authors in CST Studio Suite (2026).

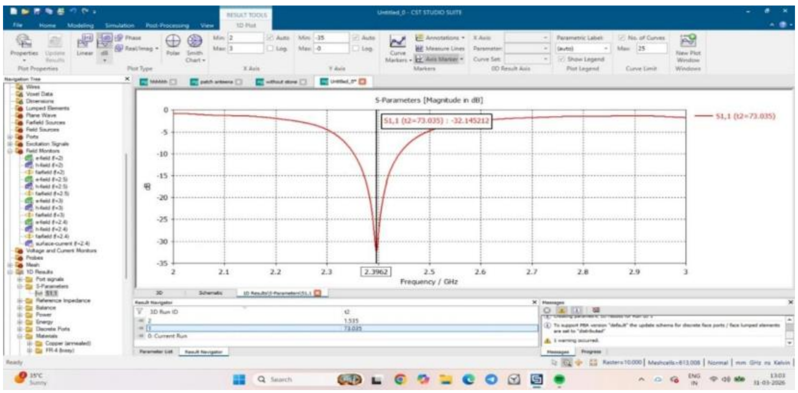

Fig. 12: S-parameter (S11) response with the stone-free kidney phantom.

Source: Simulation result generated by the authors in CST Studio Suite (2026).

International Journal of Engineering Research & Technology (IJERT)
ISSN: 2278-0181
Vol. 15 Issue 08 , August - 2026

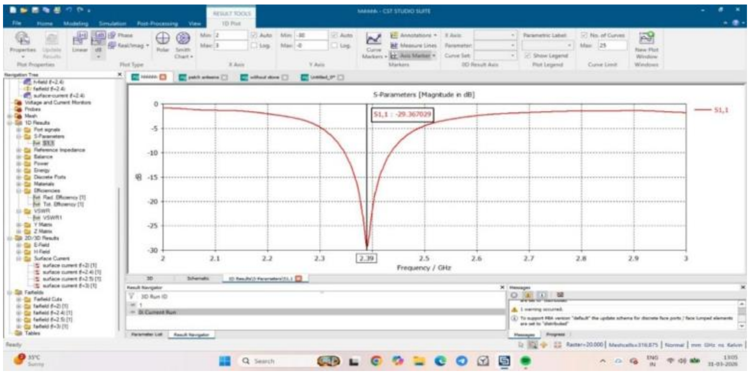

Fig. 13: S-parameter (S11) response with a kidney stone embedded in the phantom.

Source: Simulation result generated by the authors in CST Studio Suite (2026).

4.4 Comparison with Previously Reported Antennas

Table 1 places the proposed antenna alongside four previously reported renal-sensing antennas for which gain, efficiency and dimensional data are available in the literature. The comparison is restricted to designs with directly comparable, published performance figures rather than the full range of biomedical antennas discussed in Section 2, so that the comparison itself remains verifiable.

Table 1: Comparison of the proposed antenna with previously reported kidney-sensing antennas.

Ref.	Antenna Type	Dimensions (mm³)	Freq. (GHz)	Gain (dBi)	Eff. (%)	Application
[7]	Implantable monopole	14 × 10 × 0.805	0.402–0.405	—	—	Kidney cancer detection
[8]	Circularly polarised patch array	200 × 78 × 1.5	2.4	6.6	—	Kidney cancer detection
[4]	Raspberry-shaped UWB monopole	17.5 × 17.5 × 0.8	3–11	5.0	—	Kidney stone detection
[1]	Cylindrical dielectric resonator (CDRA)	π × 11 × 11 × 11	3.77	5.95	89.0	Kidney stone detection
This work	Rectangular microstrip patch	47 × 29.25 × 1.54	2.4	6.019	93.9	Kidney stone detection + WLAN

Source: compiled by the authors from [1], [4], [7], [8] and the present simulation results.

Prior single-purpose designs illustrate the trade-offs the proposed antenna aims to avoid. The implantable monopole in [7] operates in the MICS band, far from any communication standard, while the patch array in [8] achieves a comparable gain to the proposed design but at more than four times the footprint. The UWB monopole in [4] and the CDRA in [1] both target stone detection specifically but were not evaluated for WLAN compatibility. By contrast, the proposed antenna combines a comparatively compact footprint (47 × 29.25 × 1.54 mm³) with the highest reported efficiency (93.9%) among the compared designs and a gain (6.019 dBi) competitive with the larger patch array in [8], while additionally meeting 2.4 GHz WLAN impedance requirements — a combination not demonstrated together in [1], [4], [7] or [8].

On the safety side, the design recorded a Specific Absorption Rate of 1.95 W/kg under the simulated near-body placement, remaining within the 2 W/kg limit set by IEEE C95.1 for controlled exposure conditions [6]. A time-multiplexed operating scheme, in which the antenna alternates between a diagnostic mode and a communication mode rather than performing both simultaneously, is proposed as a practical way of avoiding interference between the two functions in a deployed system.

5. CONCLUSIONS

This work has designed and simulated a rectangular microstrip patch antenna intended to operate simultaneously as a 2.4 GHz WLAN element and a non-invasive kidney stone sensor. Built on an FR-4 substrate with an inset feed, the antenna achieved a free-space gain of 6.019 dBi and radiation efficiency of 93.9%, while remaining compact enough for near-body use. Evaluation against a seven-layer anatomical kidney phantom showed that the presence of a stone produces a consistent, size-dependent shift in the S11 return loss — up to 1.81 dB between the stone-free and largest-stone conditions — giving a measurable basis for microwave-based stone screening. The antenna also satisfied WLAN impedance requirements and stayed within the IEEE C95.1 SAR limit at 1.95 W/kg, indicating that the diagnostic and communication roles can, in principle, be served by the same structure through a time-multiplexed operating scheme.

These are simulation results, and several steps remain before the concept could be considered for practical deployment: fabrication and measurement of a physical prototype against a Vector Network Analyzer; testing against more anatomically detailed, and ideally tissue-mimicking, physical phantoms rather than simulated dielectric layers; and, if S11-based classification is to be automated, evaluation of the approach against a larger and more varied dataset of stone sizes and positions. Antenna array configurations for improved spatial resolution, flexible-substrate variants for wearable integration, and eventual clinical evaluation are identified as directions for continued work.

ACKNOWLEDGEMENT

The authors thank Mr. K. Srinivasa Rao, Assistant Professor (Adhoc), Department of Electronics and Communication Engineering, for his guidance throughout this project, and Dr. S. Aruna Mastani, Professor and Head of the Department, for providing the simulation facilities used in this work.

REFERENCES

[1] F. Mahbub and R. Islam, "Performance Analysis of a Cylindrical Dielectric Resonator Antenna (CDRA) for the Detection of Early-Stage Stones of the Human Kidney," in Proc. IEEE MTT-S International Microwave and RF Conference, 2022.
[2] S. B. C. Sadat and A. Hossan, "Design and Development of a Rectangular Microstrip Patch Antenna for Kidney Stone Detection and Wireless LAN Applications at 2.4 GHz," International Journal of RF and Microwave Computer-Aided Engineering, 2025.
[3] C. A. Balanis, Antenna Theory: Analysis and Design, 4th ed. Hoboken, NJ, USA: John Wiley & Sons, 2016.
[4] A. J. A. Al-Gburi et al., "A Miniature Raspberry Shaped UWB Monopole Antenna Based on Microwave Imaging Scanning Technique for Kidney Stone Early Detection," IEEE Access, 2020.
[5] M. Karthick, "Design of 2.4 GHz Patch Antennae for WLAN Applications," in Proc. IEEE National Conference on Computing and Communication Systems (NCCCIS), 2015.
[6] IEEE Standard for Safety Levels with Respect to Human Exposure to Radio Frequency Electromagnetic Fields, 3 kHz to 300 GHz, IEEE Std. C95.1-2005, 2005.
[7] I. Elshafiey, L. Shafai, and T. Almoshiqah, "Compact Implantable Monopole Antenna for Kidney Cancer Detection Using the MICS Band," IEEE Antennas and Wireless Propagation Letters, vol. 12, pp. 1–4, 2013.
[8] M. M. Islam et al., "Circularly Polarized Patch Antenna Array for Kidney Cancer Detection at 2.4 GHz," Progress in Electromagnetics Research, 2019.